

# Scaling exponents and probability distributions of DNA end-to-end distance

Francesco Valle, Mélanie Favre, Paolo De Los Rios\*, Angelo Rosa†, and Giovanni Dietler

*Laboratoire de Physique de la Matière Vivante, IPMC,*

*\*Laboratoire de Biophysique Statistique, ITP,*

*†Institut de Mathématique B,*

*École Polytechnique Fédérale de Lausanne (EPFL),*

*CH-1015 Lausanne, Switzerland*

(Dated: July 11, 2018)

## Abstract

Correlation length exponent  $\nu$  for long linear DNA molecules was determined by direct measurement of the average end-to-end distance as a function of the contour length  $s$  by means of atomic force microscopy (AFM). Linear DNA, up to 48'502 base pairs (bp), was irreversibly deposited from a solution onto silanized mica and imaged in air. Under the adsorption conditions used, the DNA is trapped onto the surface without any two-dimensional equilibration. The measured exponent is  $\nu = 0.589 \pm 0.006$ , in agreement with the theoretical 3D value of  $\nu = 0.5880 \pm 0.0010$ . The persistence length  $\ell_p$  of DNA was estimated to be  $44 \pm 3$  nm, in agreement with the literature values. The distribution of the end-to-end distances for a given contour length  $s$  and the exponents characterizing the distribution were determined for different  $s$ . For  $s$  smaller or comparable to  $\ell_p$ , a delta function like distribution was observed, while for larger  $s$ , a probability distribution of the type  $x^{d-1}x^g e^{-bx^\delta}$  was observed with  $g = 0.33 \pm 0.22$  and  $\delta = 2.58 \pm 0.76$ . These values are compared to the theoretical exponents for Self-Avoiding Walk (SAW): namely  $g = \frac{\gamma-1}{\nu}$  and  $\delta = (1-\nu)^{-1}$ . So for  $d = 2$ ,  $g \approx 0.44$  and  $\delta = 4$ , while for  $d = 3$ ,  $g \approx 0.33$  and  $\delta \approx 2.5$ . The derived entropic exponent  $\gamma$  is  $\gamma = 1.194 \pm 0.129$ . The present data indicate that the DNA behaves on large length scales like a 3 dimensional SAW.

PACS numbers: 87.64.Dz, 82.35.Gh, 87.14.Gg, 36.20.Ey

The statical properties of polymers are the focus of a strong research effort. In the limit of very long and perfectly flexible linear polymers, the situation is rather clear and the principles were laid down some time ago [1]. Self-Avoiding Walks (SAWs) describe the properties of very long polymers in 2 and 3 dimensions and the main results can be summarized in the scaling properties of polymers which were theoretically as well as experimentally confirmed [1]. Concerning DNA, the situation is more complex due to the elastic properties of the double helix, its polyelectrolytic properties and its persistence length  $\ell_p$  (see [2, 3]). Experimentally, the dynamics and statics of a purely two dimensional linear DNA chain was investigated by Maier et al. [5] finding results in agreement with the theoretical predictions. Moreover, Rivetti et al. [6] used Atomic Force Microscopy (AFM) to investigate statistical properties of DNA yielding information about the persistence length, the kinetics and the mode of adsorption on a substrate. Local changes in rigidity, curvature and/or topology of a DNA molecule induced by chemical compounds or by DNA binding proteins [7, 8, 9, 10, 11, 12] have been also studied. However, the three dimensional conformation of a flexible biopolymer is not directly delivered by the AFM, but we show here that such information can be extracted from the AFM images.

Here we present the determination of the end-to-end distance and its probability distribution as a function of the contour length  $s$  of DNA on a range spanning 4 orders of magnitude: from  $s = 1 \text{ nm}$  to  $s = 10'000 \text{ nm}$ , a range which spans values both smaller and much larger than the persistence length  $\ell_p$ . This is only possible since the atomic force microscope [13] has a very high spatial resolution but it can also image biomolecules on very larger scales. Information at the single molecule level has become available on the basis of the images of DNA molecules adsorbed onto a surface.

In the present work, the irreversible adsorption of DNA on a flat surface is investigated by measuring the mean end-to-end distance as a function of the length of the polymer contour. The experimental results show that there are two scaling regimes. At short length scales (i.e. smaller than the persistence length  $\ell_p$ ), the DNA behaves like a rigid rod. On length scales bigger than  $\ell_p$ , a 3 D behavior is observed with a Flory exponent  $\nu=0.589\pm0.006$ . Furthermore, working with images of single DNA molecules allowed us to determine the distribution of the end-to-end distances for a given contour length, an information usually unavailable. The form of the distribution depends on the flexibility of the polymer and on the contour length considered. Although several theoretical estimations of the distributions

exist [14, 15, 16], so far we are not aware of any direct experimental measurements of these parameters.

Linear DNA was prepared from a solution of  $\lambda$ -phage DNA, 48'502 base pairs (bp) long, cleaved by restriction enzymes to give a mixture of lengths from 1'503 bp up to the maximum 48'502 bp. DNA molecules were prepared in a buffer solution of 10 mM Tris-HCl, pH 7.6, 1 mM EDTA with DNA concentrations ranging from 0.5  $\mu\text{g/ml}$  to 2  $\mu\text{g/ml}$ . The Debye screening length  $1/k$  is 2 nm [18]. The substrates (freshly cleaved mica) were positively charged by exposing them to 3-aminopropyltriethoxy silane (APTES) vapors during 2 hours at room temperature in a dry atmosphere [17]. A 10  $\mu\text{l}$  drop of a DNA solution was deposited onto the substrate surface during 10 minutes and then rinsed with ultra-pure water. The sample was finally blown dry with clean air. The DNA images were recorded by means of an AFM operated in tapping mode, in order to reduce the effect of lateral forces during scanning of the surface [19]. We checked that the sample remains stable for weeks if kept in dry atmosphere, proving the irreversibility of the adsorption. In figure 1 are depicted four DNA images. From such pictures, the contour of about 60 DNA molecules was digitized using a specially designed software[20], which allows to track the molecule backbone and to extract the coordinates of the polymer contour. The first digitization, which may lead to noisy and not equidistant coordinates, was subsequently smoothed using the Snake algorithm [21]. Several tests were performed with molecules of known length (DNA plasmids) to check the procedure[20]. The analysis of the end-to-end distance  $R(s)$  for the DNA molecules as a function of the contour length  $s$  was done by moving a window of length  $s$  along the contour of the DNA molecule for values of  $s$  going from the minimal segment value  $s_{min} = 2$  nm to the total DNA length. The small values of  $s$  have a better statistical error, since they occur more often than the maximum value. The  $R(s)$  values were then averaged over all the molecules to yield the mean end-to-end  $\langle R(s) \rangle$ , which is plotted in Figure 2. One expects that  $R(s)$  scales with a single power law:

$$\langle R(s) \rangle \sim s^\nu$$

It is clear from Figure 2 that the above power law is not respected over the whole interval of  $s$ . A two power law function has to be used in order to fit the data:

$$\langle R(s) \rangle \sim \left(\frac{s}{\ell}\right)^{\nu_o} \left(1 + \frac{s}{\ell}\right)^{\nu_1 - \nu_o} \quad (1)$$

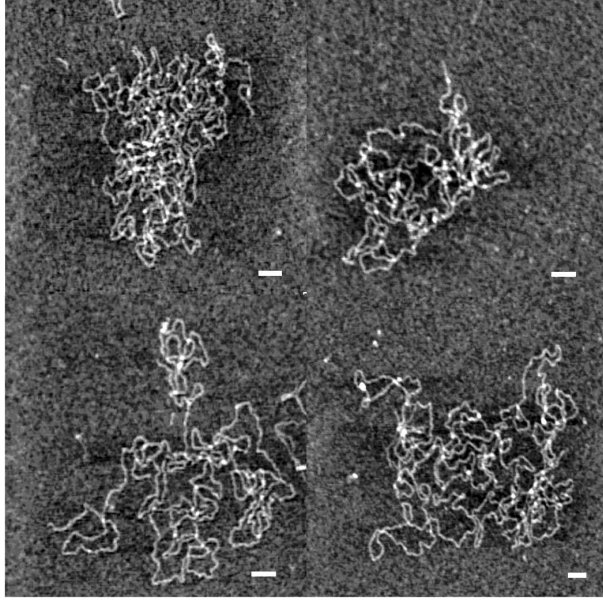


FIG. 1: a) Tapping mode images of linear DNA molecule from an enzymatic digested lambda DNA. The original DNA has 48'502 base pairs, here we show some shorter fragments. The scale bar represents 100 nm

where  $s$  is the contour length,  $\ell$  a cross-over length between the two power laws (it will be shown to correspond to the persistence length  $\ell_p$ ), and  $\nu_o$  and  $\nu_1$  the scaling (critical) exponents. The fit to the data gives the following results:

$$\nu_o = 1.030 \pm 0.017$$

$$\nu_1 = 0.589 \pm 0.006$$

$$\ell = (44 \pm 3) \text{ nm}$$

These results can be interpreted as follows. The value of  $\ell$  is in good agreement with previously reported measurements of the persistence length of DNA performed by microscopy techniques [22, 23]. We can therefore identify  $\ell$  with  $\ell_p$ , which in turn leads to a simple and intuitive interpretation of the two scaling regimes. For  $s < \ell_p$  DNA behaves as a rigid rod and the end-to-end distance scales linearly with the contour length of the polymer ( $\nu_o = 1.030$ ). For  $s > \ell_p$  the scaling exponent ( $\nu_1 = 0.589$ ) agrees with the best numerical estimations of the exponents by renormalization group techniques ( $0.5880 \pm 0.0010$  [24]) and with experimental values for synthetic polymers by scattering methods[25, 26]. Thus, the adsorbed DNA behaves as a three-dimensional polymer, which does not undergo any two-

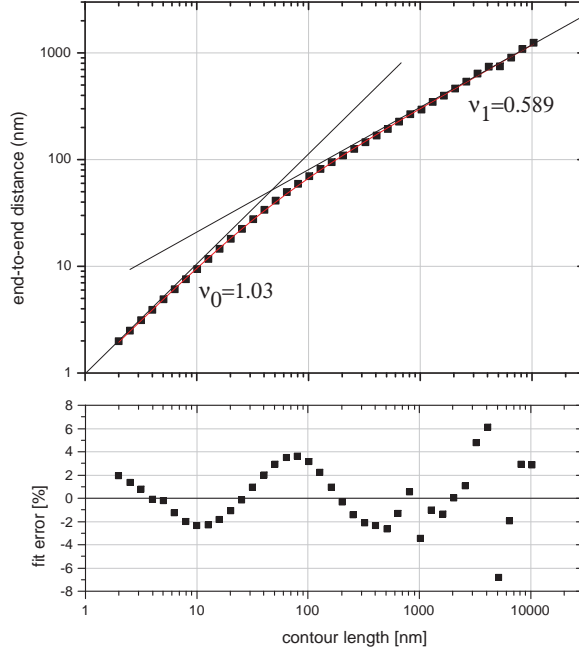


FIG. 2: Representation in double logarithmic scale of the end-to-end distance vs the contour length. Two distinct power laws are evident; the data have been fitted using equation 1.

dimensional equilibration upon adsorption. This is also evident from the images of Figure 1, where the DNA molecules show a large number of crossings. The euclidean dimension of the surface ( $d = 2$ ) onto which the molecule is projected, is larger than the fractal dimension ( $d_f = 1/\nu_1 \approx 1.7$ ) of the DNA, explaining the conservation of the 3D exponent upon adsorption on a surface [27]. We conclude that the  $\lambda$ -DNA images represent some form of a two-dimensional projection of their three dimensional bulk conformation.

Furthermore, we can measure the probability distribution of the end-to-end distance for a determined contour length  $s$  as it can be extracted from the microscopic conformation of each molecule. Two regimes are possible in respect to the persistence length:  $s \lesssim \ell_p$ , and  $s > \ell_p$ . For  $s \lesssim \ell_p$ , one expects an almost delta function distribution, since the polymer chains do not bend over these length scales. For  $s \approx \ell_p$ , the distribution is still narrow but not as peaked as for the previous case, since the molecules starts to enter the semiflexible regime: an example is given in Figure 3 for a contour length of  $s_o = 75 \text{ nm}$  ( $\approx 2\ell_p$ ). This

distribution was fitted with Winkler's equation [16]

$$f(s) = a \frac{s e^{-\frac{s_o}{8\ell_p(1-(s/s_o)^2)}}}{[1 - (s/s_o)^2] [2 - (s/s_o)^2]^2} \quad (2)$$

The fits shown in Figure 3 gives  $\ell_p = 46.6 \text{ nm}$  and  $s_o = 71.4 \text{ nm}$ , in good agreement with the literature value for the persistence length and with the nominal total length of  $75 \text{ nm}$ . For contour lengths  $s_o \gg \ell_p$ , the distribution changes dramatically and was determined for 34 different contour lengths, ranging from  $200 \text{ nm}$  to  $4'600 \text{ nm}$ . For longer contour lengths, the distributions are difficult to determine because of the reduced number of samples available and only the average end-to-end distance can be given like in Figure 1. In Figure 4 we show the distributions for  $s_o = 548 \text{ nm}$  ( $\approx 12\ell_p$ ) and  $s_o = 748 \text{ nm}$  ( $\approx 17\ell_p$ ). The histograms of figure 4 have been rescaled with  $s^{\nu_1}$  and the way they collapse onto each other is a good "*a posteriori*" confirmation of the power law previously determined (Figure 2). Starting from a SAW model [1, 29], the distribution probability of the end-to-end distance as a function of the contour length  $s$  becomes:

$$f(s) = a s^{d-1} s^\sigma e^{-bs^\delta} \quad (3)$$

The two exponents characterizing the distributions were determined from fits of the histograms for the 34 different contour lengths between  $200 \text{ nm}$  and  $4'600 \text{ nm}$ ; their averages are:

$$\sigma = 0.33 \pm 0.22$$

$$\delta = 2.58 \pm 0.76$$

These values have to be compared to those characterizing the corresponding two or three dimensional distributions of the end-to-end distances for a SAW (for  $d = 2$ ,  $\sigma = 0.44$ ,  $\delta = 4$  and for  $d = 3$ ,  $\sigma = 0.33$ ,  $\delta = 2.43$ ). The present results indicate, that the DNA chains behave like a 3 dimensional SAW.

First, it is a confirmation that in this range of DNA lengths ( $s_o \sim 5 - 100$  persistence lengths) the end-to-end distribution is matching a pure SAW distribution. Under the conditions used in our preparation, the DNA adsorption is strong and DNA is quenched on the surface. No equilibration is taking place in 2 dimensions. The problem of "trapping" or "equilibration" of DNA onto different surfaces has been already studied by Rivetti et

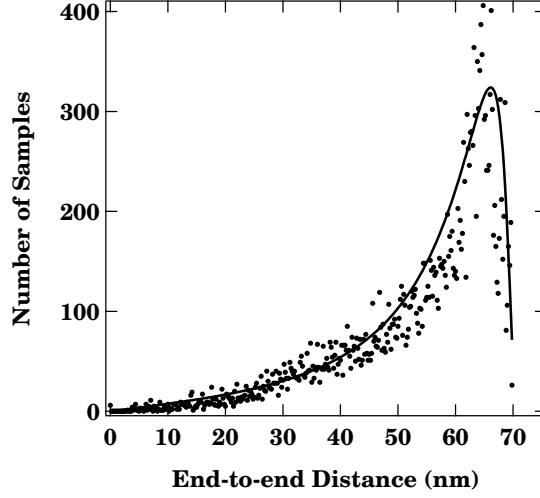


FIG. 3: Histogram representing the distribution of the end-to-end distance for a contour length  $s_0 = 75 \text{ nm}$ . The continuous line is a fit to equation 2.

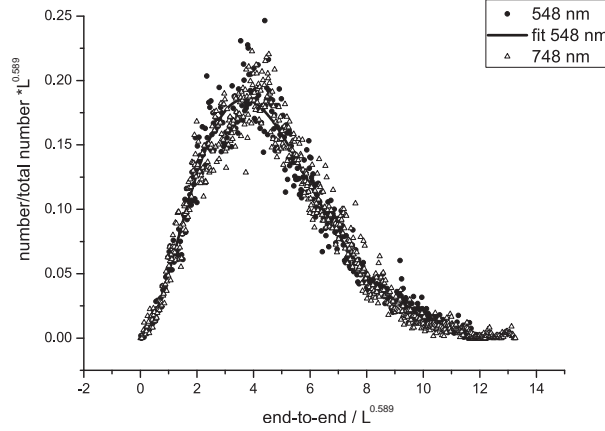


FIG. 4: Histogram representing the distribution of the end-to-end distance for two different contour length (548 nm filled circles, 748 nm open triangles) and how they collapse onto each other once they have been rescaled using the scaling exponent  $\nu_1 = 0.589$  measured in the present experiments. The solid line represents the fit of the 548 nm distribution using equation 3.

al. [6], using short DNA fragments which were then analyzed with the Worm Like Chain (WLC) model. In their work they saw large deviation from the expected three-dimensional WLC already for fragments of 6 kbp. In our work the 3D power law fits the experimental data up to  $\approx 30 \text{ kbp}$  or  $230 \ell_p$ , with no *a priori* assumption about the dimensionality of the final conformation. Compared to the optical images of fluorescently marked polymers

[5, 28], the high resolution of AFM allows to perform the analysis on segments as short as few nanometers up to 10'000 *nm* over 4 decades of lengths allowing to observe the transition from stiff to SAW polymer behavior.

Further experiments should be performed by varying the salt concentration in order to determine the contribution of the electrostatic persistence length to the total persistence length (see [3]). However, the use of high salt concentrations will also change the deposition process [6] and the adsorption might not be irreversible. A certain degree of 2 dimensional equilibration might take place, influencing the persistence length [4, 6]. Moreover, the theory of polyelectrolytes with stiffness should be used if salt and other parameters could be varied[2, 3]. In these theories a more complex behavior is predicted: a crossover from stiff rod behavior to SAW through a region of Gaussian behavior is considered. At present our data do not allow to make such a detailed test.

We would like to thank A. Stasiak, J. Prost, L. Peliti, R. Metzler, and R. Winkler for suggestions, comments and important discussions on the interpretation of the data. G.D. thanks the Swiss National Science Foundation for support through the grant Nr. 2100-063746.00.

- 
- [1] P.G. De Gennes, *Scaling Concepts in Polymer Physics*, Cornell University Press, Ithaca, 1979.
  - [2] K. Ghosh, Gustavo A. Carri, and M. Muthukumara, *J. Chem. Phys.*, **115**, 4367 (2001)
  - [3] C. Holm, J. F. Joanny, K. Kremer, R. R. Netz, P. Reineker, C. Seidel, T. A. Vilgis, and R. G. Winkler, *Adv. Polym. Sci.*, **166**, 67 (2004).
  - [4] M. Joanicot and B. Revet, *Biopolymers*, **26**, 315 (1987).
  - [5] B. Maier and J. O. Rädler, *Phys. Rev. Lett.*, **82**, 1911 (1999).
  - [6] C. Rivetti, M. Guthold and C. Bustamante, *J. Mol. Biol.*, **264**, 919 (1996).
  - [7] Y. L. Lyubchenko and L. S. Shlyakhtenko, *Proc. Natl. Acad. USA*, **94**, 496 (1997).
  - [8] C. Rivetti, C. Walker and C. Bustamante, *J. Mol. Biol.*, **280**, 41 (1998).
  - [9] Y. K. Jiao, D. I. Cherny, G. Heim, T. M. Jovin, and T. E. Shaffer, *J. Mol. Biol.*, **314**, 233 (2001).
  - [10] J. Adamcik, V. Viglasky, F. Valle, M. Antalik, D. Podhradsky and G. Dietler, *Electrophoresis*, **23**, 3300 (2002).



- [11] A. Scipioni, C. Anselmi, G. Zuccheri, B. Samori, and P. De Santis, *Biophys. J.*, **83**, 2408 (2002).
- [12] V. Viglasky, F. Valle, J. Adamcik, I. Joab, D. Podhradsky and G. Dietler, *Electrophoresis*, **24**, 1703 (2003).
- [13] G. Binnig, C. F. Quate and C. Gerber, *Phys. Rev. Lett.*, **56**, 930 (1986).
- [14] J. Wilhelm and E. Frey, *Phys. Rev. Lett.*, **77**, 2581 (1996).
- [15] D. Thirumalai and B.-Y. Ha, *cond-mat/9705200* (1997).
- [16] R. G. Winkler, *J. Chem. Phys.*, **118**, 2919 (2003).
- [17] Y. L. Lyubchenko, A. A. Gall, L. S. Shlyakhtenko, R. E. Harrington, B. L. Jacobs, P. I. Oden and S. M. Lindsay, *J. Biomol. Struct. Dyn.*, **10**, 589 (1992).
- [18] A. Vologodskii, *Macromolecules*, **27**, 5623 (1994).
- [19] R. Garcia and R. Perez, *Surf. Sci. Rep.*, **47**, 197 (2002).
- [20] J. Marek, E. Demjénová, Z. Tomori, J. Janáček, F. Valle, M. Favre and G. Dietler, *Cytometry*, **63A**, 87 (2005).
- [21] Y. Y. Wong, P. C. Yuen and C. S. Tong, *Pattern Recognition*, **31**, 1669 (1998).
- [22] J. Bednar, P. Furrer, V. Katritch, A. Z. Stasiak, J. Dubochet and A. Stasiak, *J. Mol. Biol.*, **254**, 579 (1995).
- [23] T. Berge, N. S. Jenkins, R. B. Hopkirk, M. J. Waring, J. M. Edwardson and R. M. Henderson, *Nucleic Acids Res.*, **30**, 2980 (2001).
- [24] J. C. Le Guillou and J. Zinn-Justin, *Phys. Rev. Lett.*, **39**, 95 (1977).
- [25] M. Daoud, J.P. Cotton, B. Farnoux, G. Jannik, G. Sarma, H. Benoit, R. Duplessix, C. Picot, and P.G. de Gennes, *Macromolecules*, **8**, 804 (1975).
- [26] Y. Miyaki, Y. Einaga and H. Fujita, *Macromolecules*, **11**, 1180 (1978).
- [27] B. B. Mandelbrot, *The Fractal Geometry of Nature* (W. H. Freeman and Company, Oxford, 1982).
- [28] B. Maier and J. O. Rädler, *Macromolecules*, **33**, 7185 (2000).
- [29] A. Y. Grosberg and A. R. Khokhlov, *Statistical Physics of Macromolecules* (American Institute of Physics, Woodbury, 1994).